DOI: 10.2478/cdem-2025-0007 CHEM DIDACT ECOL METROL. 2025;30(1-2):67-86

Dzheni KARADZHOVA[1], Miroslav VASILEV[1], Petya VELEVA[2] and Zlatin ZLATEV[1*]

DEFINITION OF AREAS WITH HIGH AND LOW ENVIRONMENTAL POLLUTION BY PASSIVE BIO-MONITORING

Abstract: In this work, zones with high and low air pollution were determined by passive bio-monitoring. Four classes of zones were defined, which differ in the degree of pollution. In these zones, spectral data from mulberry and linden leaves were collected. It was found that their spectral indices, reduced to three principal components using Principal Component Analysis (PCA), reflect the different levels of pollution. The relationship between the spectral indices of the leaves and the degree of pollution in the considered zones was proven using the Silhouette Method - a classification assessment technique based on cluster analysis. The present study demonstrates the possibility of passively assessing air quality based on the condition of the leaves of trees grown in urban conditions. The results obtained will support the development of continuous monitoring programs in order to control pollution and its effects.

Keywords: environmental monitoring, pollution zones, bio-monitoring, spectral indices, urban trees

Introduction

Global environmental pollution is one of the most serious challenges of the modern world, affecting not only natural ecosystems but also public health. The dimensions of the problem are many, including social, economic and legislative, and it is directly related to increasing urbanisation and industrialisation [1]. As a result of human activity and climate change, air pollution levels are reaching critical levels, which poses a significant risk to the health of the population [2]. In this regard, the search for effective and sustainable techniques for monitoring the environment, and specifically air, creates a need to address the complexity of environmental problems on our changing planet [3]. Traditional methods for monitoring changes in air quality often rely on sophisticated equipment and infrastructure, posing challenges in terms of cost, scalability and accessibility, especially in resource-limited regions [4]. In addition, in many cases, the location of monitoring stations does not reflect the real need, which leads to a misconception, most often of lower pollution values than the real ones.

In response to these challenges, attention is increasingly being paid to nature itself, seeking solutions that use the inherent abilities of living organisms to respond to changes in

[1] Faculty of Technics and Technologies, Trakia University, 38 Graf Ignatiev str., 8602, Yambol, Bulgaria, email: dzheni.karadzhova.20@trakia-uni.bg, miroslav.vasilev@trakia-uni.bg, zlatin.zlatev@trakia-uni.bg, ORCID: DK 0009-0007-5563-2813, MV 0000-0002-3859-6087, ZZ 0000-0003-3080-5048
[2] Faculty of Agriculture, Trakia University, Student's Campus, 6000 Stara Zagora, Bulgaria, email: petya.veleva@trakia-uni.bg, ORCID: PV 0000-0001-7813-6387
[*]Corresponding author: zlatin.zlatev@trakia-uni.bg

their environment [5]. Biomonitoring relies on the ability of biological organisms to reflect the state of their environment. It can be divided into two types: active and passive. In active biomonitoring, indicators are exposed in a controlled manner under different conditions, while passive biomonitoring relies on biomonitors naturally occurring in the studied areas. The first type is suitable when a high level of control over the experiment is aimed for, as the type, time and place of exposure can be chosen. In the second, the control is lower and is based on the available conditions, with the data reflecting longer-term accumulations of pollutants [6-8], indicators indicative of environmental changes related to pollution monitoring in passive biomonitoring are mainly based on bioaccumulation, biochemical changes and morphological changes in the monitored bioindicators [9].

Mulberry and linden are common in urban areas, making them potential indicator trees for passive biomonitoring. Their leaves have the ability to accumulate pollutants such as heavy metals, fine particulate matter (PM) and toxic gases, providing an opportunity to analyse pollution trends and establish their spatial distribution. A number of studies have highlighted the applicability of mulberry and linden leaves in air quality assessment, with an emphasis on their optical properties [10, 11]. They change in response to various stressors, including atmospheric pollutants, temperature fluctuations and humidity variations. Despite the successful application of leaf-level optical reflectance techniques to monitor plant responses to environmental stresses, their application in urban biomonitoring remains limited [12, 13].

The leaf surface absorbs, reflects and transmits light at different wavelengths, which makes spectral analysis possible and preferred as an indicator method for the physiological and biochemical changes occurring in tree leaves under the influence of pollutants. Nebesnyi and Grodzynska [11] state that using optical measurements, the step-by-step responses of plants to both natural and anthropogenic stress factors could be observed, which allows the diagnosis of different phases of plant adaptation and progression of pollution stress. In another study, [14], related to the deposition of atmospheric pollutants on the leaf surface of 12 tree species, it was found that the natural spectral characteristics of leaves for the purpose of air biomonitoring are closely related to the spectral response in the range 400 nm - 800 nm. The authors directly use the raw spectral features, while calculating spectral indices extracted from spectral features in the VIS region of leaves would have the potential to improve the accuracy and efficiency of air pollution biomonitoring. Using laser-induced spectroscopy in the range of 219 nm - 877 nm, Yang et al. [15] and Yu et al. [16] successfully predicted the Cu and Cr values in mulberry leaves, $R^2 = 0.98$ for both elements.

The diagnosis of airborne elements is also possible through biomonitoring based on lime leaves. In confirmation of this, using small-leaved lime leaves, a research team [17] found that high concentrations of heavy metals, especially Fe, Zn, Al and Cr, were mainly associated with road traffic, while Pb was associated with industrial pollution. The same authors diagnosed a decrease of about 27 % in the content of photosynthetic pigments in areas with high traffic and industrial pollution, a finding confirming the stress response of plants to adverse conditions.

Air quality in populated areas is a key element in the analysis of environmental and health risks posed by urbanisation and increasing industrialisation. Biological monitoring of air pollutants is becoming a vital tool for assessing the impact of air pollution on human health and the environment [18]. Mulberries and limes are tree species that respond to pollutants through changes in their anatomical and physiological properties, which can serve as indicators of environmental stress and environmental quality.

Using diagnostic signs of pollution, mainly changes in leaf pigmentation, their structure and moisture content, optical methods can help map areas with different degrees of air pollution. Techniques such as spectral and hyperspectral analysis, thermography and chlorophyll fluorescence have proven their potential in automated, objective and reproducible monitoring systems, allowing the identification and quantification of pollutants at early stages of accumulation in plant organisms [19-21]. However, existing studies on passive biomonitoring, focused on analysing the optical characteristics of tree leaves, highlight the need for new and in-depth studies of the methodologies used so far [22]. Such studies aim to improve both the efficiency and expediency of plant leaf trait assessment, thereby streamlining the integration of the obtained results into automated systems. These requirements emphasise the importance of measuring, analysing, and evaluating multiple parameters related to changes in plant traits influenced by environmental fluctuations.

Passive monitoring does not require sophisticated equipment, making it a more affordable alternative in cases where standard tools are limited by high costs or difficult-to-access locations. This method relies on naturally occurring interactions between tree leaves and the environment. As a result, it is possible to assess not only current pollution, but also to predict future changes in environmental conditions related to anthropogenic or climatic factors. Through non-invasive optical monitoring and the use of spectral indices, it is possible to accurately assess the extent of pollution, as well as its impact on plant indicators. This contributes to improving biomonitoring strategies and provides more effective methods for assessing air quality in urbanised and industrial areas.

The aim of this work is to define areas with high and low air pollution from the perspective of passive bio-monitoring.

Material and methods

The study measured key parameters related to air pollution: concentrations of fine particulate matter (PM2.5 and PM10), total volatile organic compounds (VOC), equivalent carbon dioxide (eCO_2), as well as concentrations of nitrogen oxides (NO_x), sulphur oxides (SO_x), and carbon monoxide (CO). These indicators are essential when aiming to obtain accurate results when assessing air quality, as each of them plays a role in different aspects of pollution and their impact on the environment and human health. The measurement object is also the leaves of lime trees (*Tilia platyphyllos*) and mulberries (*Morus alba*), common trees in urban and suburban environments.

Table 1

Geographic coordinates of measurement areas, according to the degree of pollution

Measurement area	Geographic coordinates (WGS 84)
Z1	42.475868N, 26.518947E
Z2	42.474494N, 26.522722E
Z3	42.490862N, 26.459554E
Z4	42.490190N, 26.511425E
Z5	42.418299N, 26.932481E
Z6	42.501629N, 26.528357E

Table 1 presents the data on the areas from which the leaves were taken. The pollution levels and geographical coordinates are indicated. The area is located in the southeastern part of Bulgaria. The population of mulberries and lime trees in the studied geographical region is significant.

Passive determination of environmental characteristics based on data from the leaves of the studied plants corresponds to passive biomonitoring in this case.

Figure 1 presents the measurement zones on a satellite image. Zones 1, 2, 3 and 4 are located in the urban area, zone 6 is in an area outside the city, and zone 5 is located in a settlement 40 km away from the city.

Measurements in highly and less urbanised areas are dictated by the need to cover a wide range of environmental conditions, which allows for a more accurate assessment of the impact of pollution on different types of environments.

Fig. 1. Measurement zones on a satellite image (images are property of Google Inc.)

The criteria for determining the high and low level thresholds for the relevant pollutants are presented in Table 2. These threshold levels are defined by WHO, EPA and are reported in various literature sources.

Table 2

Criteria for determining threshold levels of pollutants

Pollutant	Threshold value	Criteria	Source
PM2.5	35 μg/m^3	Levels above 35 μg/m^3 are considered high according to health guidelines (e.g. WHO, EPA) for 24-hour average exposure	[23]
PM10	50 μg/m^3	Levels above 50 μg/m^3 are considered high based on 24-hour average exposure guidelines	
VOC	1 ppm	Total volatile organic compound levels above 1 ppm are considered high and may indicate poor air quality	[24]
eCO_2	410 ppm	CO_2 equivalent levels above 410 ppm are considered high, indicating poor air quality	[25]
NO_x	1 ppm	Nitrogen oxide levels above 1 ppm are considered high and may have adverse health effects	[26]
SO_x	0.6 ppm	Sulphur oxide levels above 0.6 ppm are considered high, with potential health consequences	[27]
CO	0.6 ppm	Carbon monoxide levels above 0.6 ppm are considered high, which is a health risk	[28]

The environmental characteristics were determined with a measuring device developed at FTT-Yambol, Bulgaria [29].

Figure 2 shows images of mulberry and linden leaves - upper and lower sides. The adaxial (upper) surface and abaxial (lower) surface of the leaves were analysed.

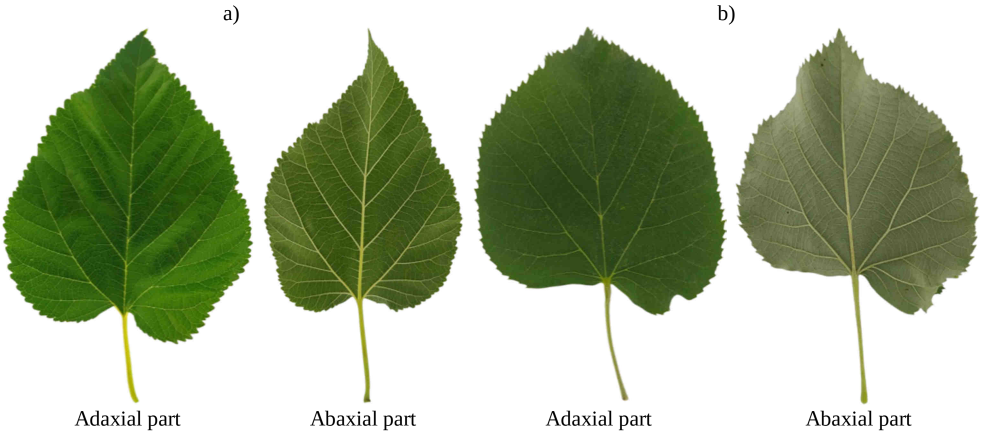

Fig. 2. Images of: a) mulberry and b) linden leaves showing both adaxial (upper) and abaxial (lower) surfaces, which were analysed for spectral indices

Obtaining spectral characteristics in the VIS spectral range. The full spectrum of the images was used in obtaining VIS spectral characteristics. The conversion functions are for observer 2o (Stiles and Burch 2o, RGB (1955)) and illumination D65 (average daylight with UV component (6500 K)), according to mathematical relationships, in which the conversion is possible in both directions of the equality [30].

Calculation of spectral indices. Spectral indices were used [31, 32]. The indicated wavelengths are in the visible range of the spectrum. The indices were calculated: REI, PTI, CTI, TVI, G, NExG, NGRDI, RGBVI, GLI, VARI and ExG. A vector of features was formed from them.

Data reduction in feature vectors. The feature vector data was reduced using Principal Component Analysis (PCA) [33]. This is a statistical technique for dimensionality reduction. It works easily with large data sets by transforming them into a smaller set of variables, called principal components, each of which is a linear combination of the original variables, ordered by the amount of variance it captures in the data.

All data were processed at a significance level of $\alpha = 0.05$.

A check was made for the separation of classes covering areas with different degrees of environmental pollution using a classification procedure based on cluster analysis. The "*S*" criterion was used, determined using the Silhouette function in the Matlab (The Mathworks Inc., Natick, MA, USA) environment. Unlike most procedures for evaluating the effectiveness of clustering, Silhouette does not require a preliminary set of training data to provide reliable results for grouping classes, but focuses entirely on the internal characteristics of the data. Table 3 presents the stages of the check using Silhouette analysis.

Table 3

Stages of Silhouette analysis

Stage	Description	Meaning
E1	Data reduction	Reduction of the volume of spectral data, describing a significant part of their variance
E2	Visualisation	Visualisation of potential clusters and their overlap
E3	k-NN clustering	Verification of the separability of the formed classes according to pollution using a basic classifier. Finding overlapping classes by visual assessment
E4	Silhouette Score	Quantitative measure of the separability of the classes. High values indicate good separability, low and negative values - partial overlap of data distributions

Three distance functions are used in k-NN clustering:

- **sqEuclidean (*SE*)**. It represents the Euclidean distance raised to the second power. It is calculated using the following formula:

$$SE = \sum_{i=1}^{n} (x_i - y_i)^2 \qquad (1)$$

where *x* and *y* are the data in the vectors being compared; *n* is the length of the data vector.

- **cityblock (*CB*)** or Manhattan distance. It is calculated by the following formula:

$$CB = \sum_{i=1}^{n} |x_i - y_i| \qquad (2)$$

To calculate **cosine (*CS*)**, we use the equation:

$$CS = 1 - \frac{\sum_{i=1}^{n} x_i y_i}{\sqrt{\sum_{i=1}^{n} {x_i}^2} \times \sqrt{\sum_{i=1}^{n} {y_i}^2}} \qquad (3)$$

- the "*S*" criterion of the Silhouette method is calculated by the following formula:

$$S = \frac{b_i - a_i}{\max(a_i, b_i)} \qquad (4)$$

where *i* is the number of data in both clusters; a_i is the average distance from the *i*-th point to the other points in the same cluster; b_i is the minimum average distance from the *i*-th point to the points in the other clusters. If the *i*-th point is the only point in the corresponding cluster, then the silhouette value "*S*" is taken as 1. The value of *S* is a dimensionless quantity and can be taken as a relative unit (a.u.).

The values of the silhouette "*S*" vary from [–1;1]. If "*S*" tends to 1, it indicates that the corresponding point lies in its own cluster and does not coincide with the other clusters. If "*S*" has values tending to 0 or negative, this is an indication of overlap between the clusters. If $S = 0$, the points are borderline between the clusters, and it cannot be clearly defined to which of the clusters they belong [34].

The cluster silhouette plot visualises the silhouette values for each point. Points with high silhouette values are located on the right side of the plot, indicating strong clustering, while points with low values appear on the left, indicating weaker clustering.

The average silhouette value "*S*" for all points is an overall measure of the quality of clustering of the data into clusters. For a correct interpretation of the results obtained, the following threshold values were adopted [35]:

1. If $S > 0.7$. The data fitting into their corresponding clusters is high. The separation between classes is also defined as high.

2. If $0.51 \leq S \leq 0.70$. A significant part of the data is correctly classified into their corresponding cluster. Moderate separation between classes is observed.
3. If $S < 0.5$. Significant overlap of data distributions, leading to data being placed in the wrong cluster. Clustering results are unsatisfactory.

Results

The measurement areas are divided into four classes, depending on the levels of PM and the degree of contamination by the other pollutants measured. The division is made according to whether the respective pollutant is below or above the threshold value. The threshold values and pollution levels are presented in Table 4.

Table 4

Threshold levels of pollutants and pollution levels of measurement areas

Measurement zone	**PM2.5**	**PM10**	**VOC**	**eCO_2**	**NO_x**	**SO_x**	**CO**
Threshold value	**35 µg/m³**	**50 µg/m³**	**1 ppm**	**410 ppm**	**1 ppm**	**0.6 ppm**	**0.6 ppm**
Z1	H	H	L	L	H	H	H
Z2	H	H	H	L	L	L	L
Z3	H	H	L	L	L	L	L
Z4	L	L	L	H	L	L	H
Z5	L	L	H	H	H	H	H
Z6	L	L	L	L	L	L	L
H - high level of contaminant; L - low level of contaminant							

The resulting four classes of zones with different degrees of contamination are presented in Table 5. Classes 1 and 3 cover one zone each, while classes 2 and 4 have two zones each.

Table 5

Grouping of measurement areas into classes, depending on the degree of pollution

Class	**Degree of contamination**	**Measurement zones**
Class C1	H-PM, HLP	Z1
Class C2	L-PM, LLP	Z2, Z3
Class C3	L-PM, HLP	Z5
Class C4	L-PM, LLP	Z4, Z6
H-PM - high levels of fine particulate matter; L-PM - low levels of fine particulate matter; HLP - high levels of other pollutants; LLP - low levels of other pollutants		

Table 6 shows the average values of pollutants in the four classes. The pollutant data highlight clear contrasts between the four classes, with 1 and 2 being the most polluted, especially in terms of fine particulate matter (PM2.5, PM10) and VOC, an indication of emissions from heavy industry and vehicles. Class 1 has the highest values of NO_x and SO_x, indicative of its proximity to intensive or industrial areas, while class 2 has the highest concentration of VOC. On the other hand, class 4 shows the lowest values of all pollutants, reflecting lightly polluted areas, such as rural or suburban areas. Class 3 occupies an intermediate position; the levels are relatively moderate for eCO_2 and VOC, highlighting suburban areas with average levels of harmful emissions.

Table 6

Measured values of pollutants in the four classes of zones (all data have a statistically significant difference at $p < 0.05$)

Class \ Pollutant	PM2.5 [μg/m^3]	PM10 [μg/m^3]	VOC [ppm]	eCO_2 [ppm]	NO_x [ppm]	SO_x [ppm]	CO [ppm]
Class 1	45 ±82	60 ±90	2.07 ±0.63	401.6 ±6.4	0.88 ±0.13	1.00 ±0.03	0.70 ±0.08
Class 2	128 ±98	143 ±106	6 ±13	403 ±16	0.83 ±0.33	0.57 ±0.07	0.50 ±0.04
Class 3	16.6 ±3.5	28.5 ±9.4	4.0 ±1.0	448 ±41	0.79 ±0.12	0.57 ±0.03	0.73 ±0.01
Class 4	5.1 ±5.5	18.1 ±9.8	1.02 ±0.70	409 ±14	0.57 ±0.09	0.51 ±0.03	0.60 ±0.02

According to the adopted standardised criteria for threshold levels of environmental pollutants, the following vector of features has been defined:

$$FVT = [PM2.5\ PM10\ VOC\ eCO_2\ NO_x\ SO_x\ CO] \quad (5)$$

Figure 3 visualises the four classes, based on data from the feature vector, covering the measured air quality parameters, reduced to three principal components using Principal Component Analysis (PCA). Some of the partial overlap of data distributions, because not all characteristics in the respective class have low or high levels relative to their threshold value.

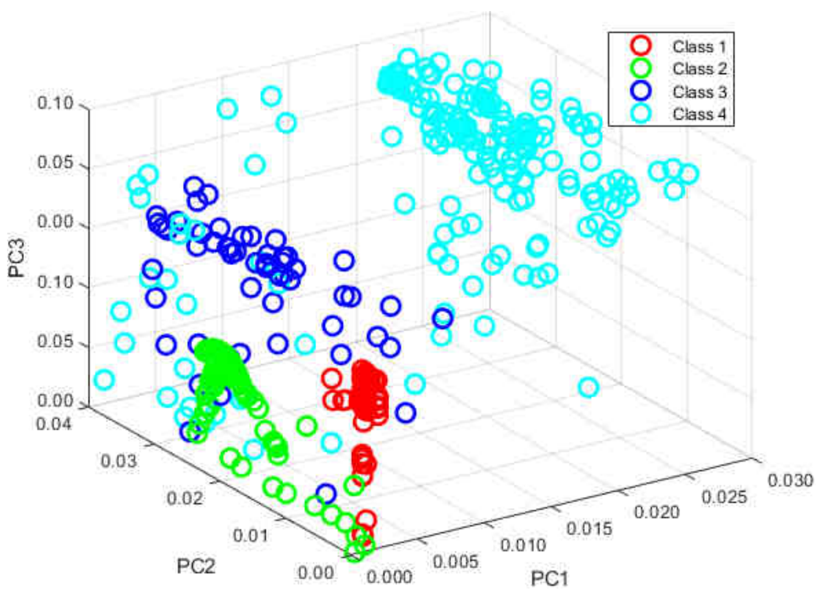

Fig. 3. Principal Component Analysis (PCA) visualisation of feature vector data (PM2.5, PM10, VOC, eCO_2, NO_x, SO_x, CO), reduced to three principal components to illustrate separation between pollution classes. All data are dimensionless

Figure 4 shows graphs for the separability of the four classes into clusters.

The graphs show that the worst clustering is obtained when using cityblock distance (*CB*). The best indicators of the Silhouette value are observed in cluster analysis based on cosine distance (CS), in which visually a very small part of the data in cluster 3 overlaps with the rest of the data. With Euclidean distance, an overlap of part of the data for cluster 3 with the rest of the clusters is visible.

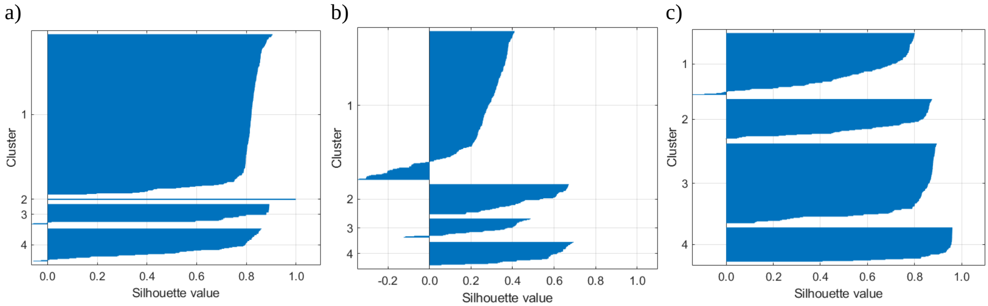

Fig. 4. Separability of the four pollution classes using three distance functions: a) sqEuclidean, b) cityblock, c) cosine. Higher Silhouette values indicate stronger clustering. All data are dimensionless

Table 7 presents results for the coefficient "*S*" when dividing the four classes of areas with different degrees of environmental pollution.

Table 7

S-values between classes according to the air quality characteristics. [-] all data are dimensionless

Distance function	sqEuclidean			cityblock			cosine		
Basic statistics / Classes	min.	max.	mean	min.	max.	mean	min.	max.	mean
c1-c2	0.09	1.00	**0.97**	0.02	0.76	**0.66**	–0.06	0.84	**0.62**
c1-c3	–0.50	0.99	**0.91**	0.16	0.87	**0.78**	0.06	0.95	**0.74**
c1-c4	–0.50	0.99	**0.91**	–0.63	0.87	**0.25**	0.09	0.96	**0.88**
c2-c3	–0.11	0.93	**0.82**	–0.18	0.73	**0.53**	0.00	0.80	**0.58**
c2-c4	–0.09	0.94	**0.84**	–0.23	0.79	**0.69**	0.02	0.89	**0.70**
c3-c4	–0.13	0.88	**0.69**	–0.18	0.82	**0.47**	0.01	0.88	**0.70**
c1-c2-c3-c4	–0.49	0.87	**0.64**	–0.14	0.66	**0.48**	–0.14	0.96	**0.73**

In order to more accurately determine the boundaries between closed classes and how clearly they are distinguished from each other, the clustering using the Silhouette method was evaluated, both between individual pairs of studied classes and for all of them simultaneously. This approach provides an opportunity for a more precise analysis of the overall structure of the data and their interpretation within the classes.

The squared Euclidean distance provides the best separability, with the highest average silhouette values in most pairs of classes. More significant overlap is observed in the clustering, aiming at separability between all classes simultaneously, 0.6.

The cosine distance shows moderate separability, with the highest values being between c1-c4, the pair of classes differing most in the degree of contamination. With a value of the *S* criterion of 0.73, this distance function demonstrates the best results in the sought separability between the four defined classes.

The *CB* distance presents the weakest overall separability, especially for the pair c1-c4, where significant overlap is indicated by the negative minimum silhouette value and the low mean value, 0.25. The mean silhouette value at separability of all classes with this distance function falls in the low range of separability, 0.4.

A vector containing 11 spectral indices of mulberry leaves is formed. The data are separate for the upper and lower parts of the leaves. This vector has the form:

$$FVM = [REI\ PTI\ CTI\ TVI\ G\ NExG\ NGRDI\ RGBVI\ GLI\ VARI\ ExG] \quad (6)$$

Figure 5 visualises data for mulberry leaves. Although there is overlap between classes, due to close values in some of the indicators, they are still grouped. Visually, a more significant overlap is observed between the underside of the leaves, an aspect that will be verified by applying the selected clustering method.

a) b)

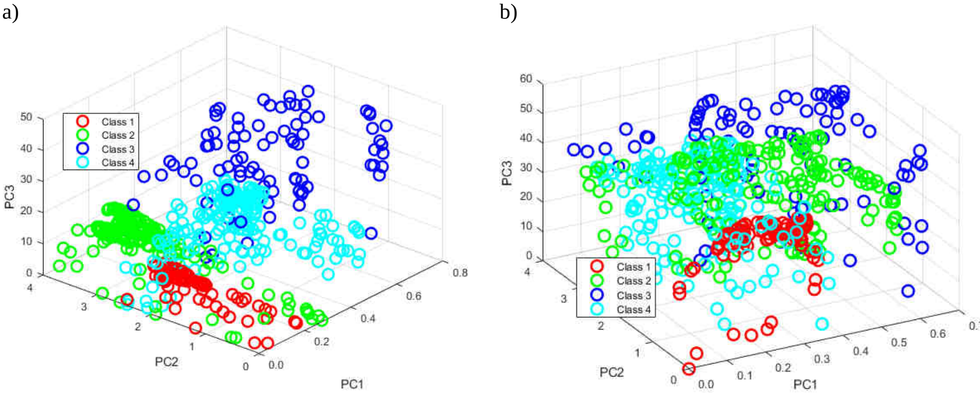

Fig. 5. Principal components of mulberry leaves (adaxial (a) vs. abaxial (b) surfaces) across four pollution classes. Overlaps between classes are visible, particularly in the abaxial data

Figure 6 shows graphs of the separability of the four classes into clusters. The data are for mulberries from the upper side of the leaves.

a) b) c)

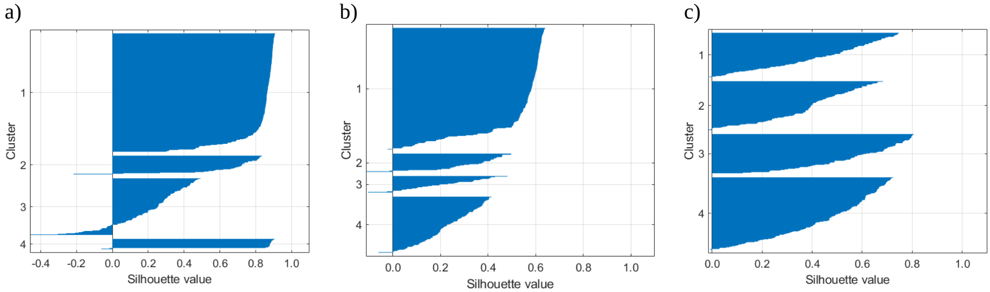

Fig. 6. Separability of pollution classes based on spectral indices of the adaxial (upper) surface of mulberry leaves, using: a) sqEuclidean, b) cityblock, and c) cosine distance functions

The graphs show that all three distance functions have positive values of the Silhouette criterion, an indicator of good grouping of data in the respective clusters. Visually, only when applying Euclidean distance does a small portion of class 1 data points become misclassified into other clusters. Classes 2 and 3 with the *CB* function show the lowest average values of the *S* criterion, up to about 0.5.

Table 8 presents results for the "*S*" coefficient when dividing the four classes of areas with different degrees of environmental pollution.

Table 8

S-values between classes according to the adaxial part of mulberry leaves. [-] all data are dimensionless

Distance function	sqEuclidean			cityblock			cosine		
Classes \ Basic statistics	min.	max	mean	min.	max	mean	min.	max	mean
c1-c2	0.03	0.90	**0.79**	–0.23	0.66	**0.46**	0.01	0.88	**0.71**
c1-c3	–0.38	0.93	**0.52**	–0.02	0.76	**0.66**	0.02	0.91	**0.76**
c1-c4	–0.09	0.93	**0.84**	–0.07	0.76	**0.65**	0.00	0.82	**0.58**
c2-c3	–0.36	0.89	**0.46**	–0.24	0.70	**0.49**	0.00	0.84	**0.59**
c2-c4	–0.12	0.90	**0.78**	–0.17	0.65	**0.44**	0.02	0.82	**0.62**
c3-c4	–0.33	0.84	**0.59**	–0.27	0.55	**0.34**	0.01	0.84	**0.65**
c1-c2-c3-c4	–0.17	0.76	**0.54**	–0.04	0.75	**0.43**	–0.03	0.78	**0.47**

The quantitative assessment of the separability between classes with data obtained from the upper side of mulberry shows that using sqEuclidean, a moderate to high average value of "*S*" is observed between pairs of classes. This is an indication of good separability and a clear distinction between them. Clustering, involving the simultaneous use of all classes and its evaluation by the "*S*" criterion, indicates moderate separability between classes, due to overlap between classes within the more complex structure of the data. However, sqEuclidean provides the best separability between 4 classes compared to the other two distance metrics. The obtained average values of "S" for the pairs c1-c3, c2-c3 and c3-c4 indicate higher separability for the cosine distance, while for the remaining pairs, the discriminability is lower compared to that obtained with sqEuclidean. The *CB* distance presents the weakest overall separability, especially for the c3-c4 pair, where significant overlap is indicated by the negative minimum silhouette value and the low mean value, 0.34.

Figure 7 shows separability plots for the four classes in clusters. The data are for mulberries on the underside of the leaves.

a)

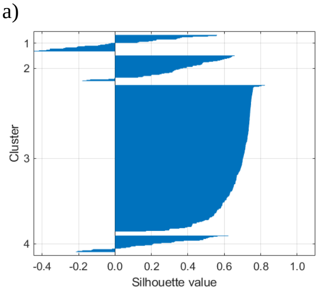

b)

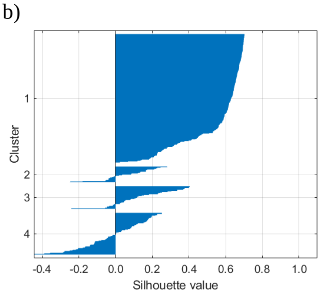

c)

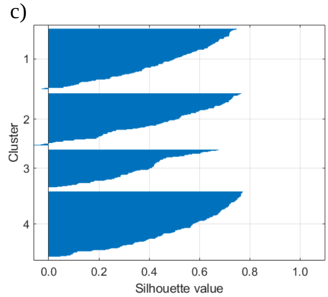

Fig. 7. Separability of the classes according to the abaxial part of mulberry leaves, using: a) sqEuclidean, b) cityblock, and c) cosine distance functions

The presented plot of class separability with data in clusters using sqEuclidean shows that a small part of the spectral data for classes C2, C3 and C4 fall incorrectly into the others. Positive values of the coefficient “*S*” are an indication of good overall separability of the data in their respective clusters. A significantly less accurate distinction between the classes covering the different pollution zones is visualised at the distance *CB*. The separation of these classes is not clearly expressed, which is a result of the similarity in the characteristics of the data between the respective clusters, visualised by the negative values of the silhouette. However, the impact of these values on the overall mean value of the silhouette may be minimal if the misclassified points are a small part of the total data volume. Quantitative assessment would provide a more detailed picture of what part of the data is misclassified. The cosine function presents a high degree of clustering, confirmed by its Silhouette graph, for all classes, above 0.7.

Table 9 presents results for the coefficient “*S*” when dividing the four classes of areas with different degrees of environmental pollution.

Table 9

S-values between classes according to the abaxial part of mulberry leaves

Distance function	**sqEuclidean**			**cityblock**			**cosine**		
Basic statistics / Classes	**min.**	**max**	**mean**	**min.**	**max**	**mean**	**min.**	**max**	**mean**
c1-c2	–0.36	0.89	**0.72**	–0.22	0.68	**0.49**	0.02	0.86	**0.69**
c1-c3	–0.40	0.91	**0.75**	–0.06	0.55	**0.36**	0.00	0.86	**0.70**
c1-c4	–0.40	0.84	**0.64**	–0.07	0.44	**0.26**	0.01	0.84	**0.62**
c2-c3	–0.23	0.82	**0.59**	–0.02	0.68	**0.52**	0.01	0.85	**0.61**
c2-c4	–0.10	0.87	**0.58**	–0.20	0.69	**0.52**	0.05	0.90	**0.69**
c3-c4	–0.17	0.87	**0.68**	–0.17	0.64	**0.53**	0.02	0.85	**0.67**
c1-c2-c3-c4	–0.46	0.75	**0.49**	–0.42	0.60	**0.27**	0.00	0.79	**0.47**

The quantitative assessment of class separability shows average values of the criterion “*S*” between individual classes using the sqEuclidean and *CS* distance functions in the range from 0.58 to 0.75. As expected, the silhouette value is lower for the overall class discriminability: 0.49 and 0.47. Clustering based on the *CB* function has the lowest values of “*S*”, a sign of limited efficiency in distinguishing classes with high heterogeneity. This is especially clearly noticeable when examining the possibility of classification of all formed classes. The average value of “*S*” is 0.27.A vector containing 11 spectral indices of a linden leaf was formed. The data are separate for the upper and lower parts of the leaves.

This vector has the form:

$$FVA = [REI\ PTI\ CTI\ TVI\ G\ NExG\ NGRDI\ RGBVI\ GLI\ VARI\ ExG] \quad (7)$$

Figure 8 visualises data for linden leaves. The classes indicating different degrees of air pollution are largely overlapping. A compact grouping of the data is observed for the underside of linden leaves, as well as for classes 2 and 4 on the upper side. It is necessary to perform a separability check to establish the potential of the spectral indices obtained from linden, in order to define areas with different pollution.

Figure 9 shows graphs of the separability of the four classes into clusters. The data are for linden from the upper side of the leaves. From the graphs presenting the value of Silhouette, it is seen that it has the highest values in the cluster analysis using sqEuclidean and *CS* distance. In these cases, visually, the value of the “*S*” criterion is above 0.7 for all classes. The use of *CB* in the clustering task also shows negative values for classes C3 and

C4, a sign of overlap with the other classes. With lower values of the silhouette are also its positive values, not exceeding 0.6.

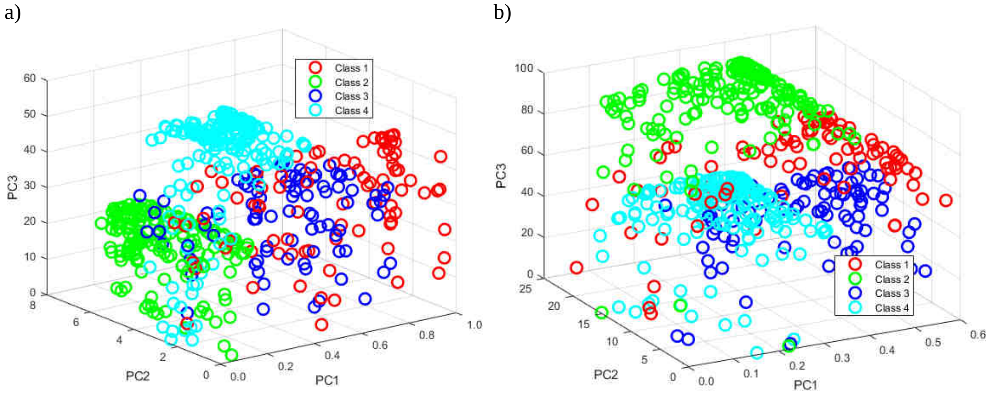

Fig. 8. Linden leaf data visualisation (adaxial (a) vs. abaxial (b) surfaces)

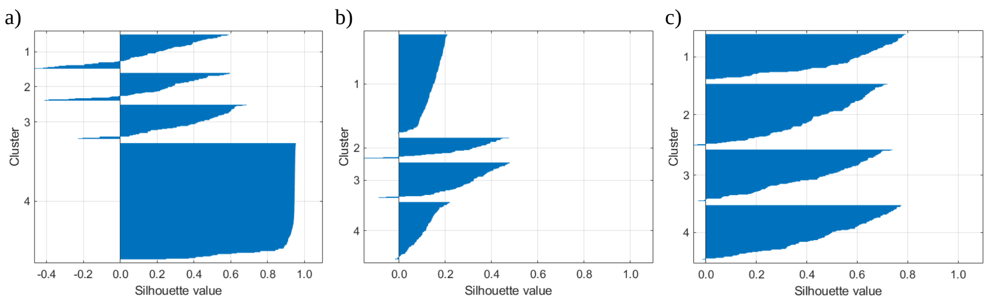

Fig. 9. Separability of the classes according to the adaxial part of linden leaves, using: a) sqEuclidean, b) cityblock, and c) cosine distance functions

Table 10 presents the results for the coefficient "*S*" when dividing the four classes of areas with different degrees of environmental pollution.

Table 10

S-values between classes according to the adaxial part of linden leaves

Distance function	**sqEuclidean**			**cityblock**			**cosine**		
Basic statistics / Classes	**min.**	**max**	**mean**	**min.**	**max**	**mean**	**min.**	**max**	**mean**
c1-c2	–0.11	0.92	**0.82**	–0.10	0.78	**0.67**	–0.01	0.76	**0.62**
c1-c3	–0.25	0.90	**0.76**	–0.02	0.57	**0.42**	0.01	0.83	**0.68**
c1-c4	–0.02	0.86	**0.71**	–0.10	0.71	**0.57**	–0.01	0.80	**0.60**
c2-c3	–0.12	0.92	**0.81**	–0.06	0.77	**0.66**	0.00	0.81	**0.59**
c2-c4	–0.25	0.79	**0.65**	–0.06	0.74	**0.61**	0.02	0.87	**0.62**
c3-c4	–0.03	0.86	**0.70**	–0.12	0.68	**0.55**	0.00	0.84	**0.68**
c1-c2-c3-c4	–0.04	0.87	**0.68**	–0.13	0.59	**0.41**	–0.06	0.81	**0.51**

The highest average values of the “*S*” criterion are the separability achieved with the sqEuclidean function, above 0.65 for all considered pairs of classes. Distinctions with lower maximum and average values are visualised with *CS* distance, and those obtained between classes c1-c3 and c3-c4 can be considered sufficiently accurate from the point of view of the classification task. As in the data considered so far for defining areas with different pollution, the lowest values of the “*S*” criterion, showing strong overlap in the data, are obtained with clustering using the *CB* distance. The exception is the separability between classes c1-c2 and c2-c3, with an “*S*” value higher than 0.65. In the general clustering, including all four classes, the average value of the “*S*” criterion is the highest with sqEuclidean, 0.68, while with *CS* it can be defined as moderate, 0.51. The *CB* distance function again has the lowest value of the silhouette, 0.41.

Figure 10 shows the separability graphs of the four classes into clusters. The data are for linden on the underside of the leaves.

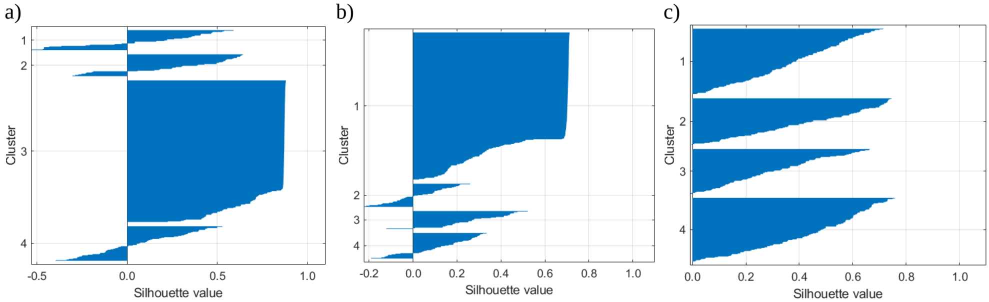

Fig. 10. Separability of the classes according to the abaxial part of linden leaves, using: a) sqEuclidean, b) cityblock, and c) cosine distance functions

The tendency to visualise significantly lower values of “*S*”, observed in the clustering with data obtained from the underside of the mulberry leaf compared to the upper side, is also preserved in the classes containing spectral indices of lime. The negative values of the silhouette, observed in the quadratic Euclidean and *CB* distances for some of the classes, indicate overlapping data in the clusters. In the cluster analysis using the *CS* function, the classes are well-defined with a value of the “*S*” criterion reaching about 0.7.

Table 11 presents the results for the coefficient “*S*” when dividing the four classes of areas with different degrees of environmental pollution.

Table 11

S-values between classes according to the abaxial part of linden leaves. [-] all data are dimensionless

Distance function	**sqEuclidean**			**cityblock**			**cosine**		
Basic statistics / Classes	**min.**	**max**	**mean**	**min.**	**max**	**mean**	**min.**	**max**	**mean**
c1-c2	–0.12	0.87	0.73	0.01	0.73	0.60	–0.01	0.81	0.58
c1-c3	–0.21	0.84	0.67	–0.22	0.67	0.51	0.05	0.80	0.58
c1-c4	–0.34	0.91	0.76	–0.02	0.66	0.52	0.00	0.84	0.63
c2-c3	–0.10	0.80	0.61	–0.25	0.62	0.35	–0.01	0.82	0.60
c2-c4	–0.06	0.77	0.56	–0.22	0.66	0.50	0.01	0.83	0.62
c3-c4	–0.17	0.90	0.76	–0.16	0.71	0.57	0.00	0.85	0.63
c1-c2-c3-c4	–0.47	0.86	0.59	–0.35	0.84	0.49	0.00	0.74	0.42

The discriminability between pairs of classes using squared Euclidean distance shows moderate to high separability, based on the average value of the "*S*" criterion. It is lowest among classes C2-C4, and highest for the strongly different in their pollution value classes C1-C4, 0.76. Moderate separability is characterised by the results obtained for clustering with *CB* and *CS* distance functions, where the value of Silhouette does not exceed 0.63. The average values of "*S*" for the separability of four classes are from 0.42 with the *CS* function to 0.59 in the cluster analysis using squared Euclidean distance.

Figure 11 shows a summarised diagram of the values of the "*S*" criterion for separability between classes using the environmental parameters, upper and lower sides of mulberry and linden leaves, depending on the distance function used in the cluster analysis.

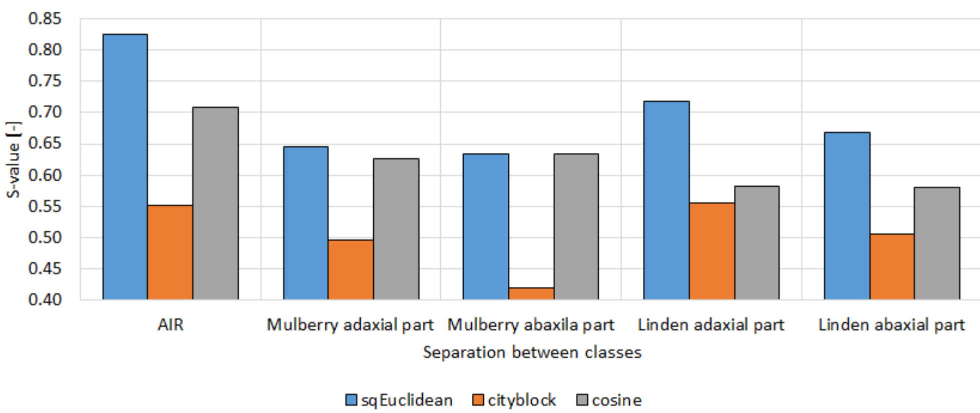

Fig. 11. Summary diagram of *S*-values

In terms of the data used to perform class separation, covering different areas of pollution, the directly obtained pollution values (AIR class) with the highest predictive ability are. In addition to the data used, the distance function used to perform the cluster analysis also has an impact on the accuracy of separation. Higher values, above 0.6, are visualised when applying the sqEuclidean metric. This is seen in all data used except those obtained from the underside of mulberry, where the accuracy is comparable to that obtained using the *CS* function. The cosine distance provides moderate separation (from 0.58 to 0.71), with consistent *S*-values across samples, although it does not reach the efficiency of the Euclidean square. The *CB* (Manhattan) distance shows the lowest *S*-values, especially for the underside of mulberry and lime leaves, which indicates significant overlap and poor distinction between classes.

Based on the "*S*" criterion, lindens are more informative in defining areas with different pollution. The data obtained from the upper side of the leaves of these plants shows a silhouette value above 0.7. In both plant species, the spectra obtained from the upper side of the leaves provide a higher predictive ability. This is especially clear in the case of linden leaves.

Discussion

The four defined classes represent different areas with different levels of pollution. These classes are determined based on proximity to industrial areas, traffic density, or rural versus urban environments.

Class 1 shows elevated levels of multiple pollutants, particularly PM2.5, PM10, NO_x, and SO_x. This indicates a heavily polluted area, likely near industrial sites or heavily trafficked urban areas.

Class 2 has the highest levels of particulate matter (PM2.5 and PM10) and VOCs, suggesting an area with significant industrial emissions or heavy vehicle pollution. This may represent an industrial or densely populated urban area.

Class 3 shows moderate pollution, with higher levels of eCO_2 and VOC compared to other areas. This may represent a moderately polluted area, such as a suburban area with moderate vehicle or industrial emissions.

Class 4 includes the lowest pollution areas, with the lowest levels of most pollutants. It likely represents rural or low-density areas with minimal industrial or traffic-related pollution.

The class distinction, carried out in order to correctly define areas with different pollution, shows that AIR data presents a higher classification accuracy, compared to the spectral indices obtained from lime and mulberry. This is an expected result, given that, in this way, data is provided that directly reflects the physical and chemical properties of pollutants in the studied areas. Spectral data from leaves is an indirect indicator of pollution and can be influenced by many external factors, leading to lower predictive abilities. In this regard, Khavanin Zadeh et al. [12] found that the direct use of spectral features for passive determination of air pollution is more effective when using lime leaves and less effective for mulberry. They explain the obtained results with the species specificity of the physiological and structural responses of tree leaves to the quality of habitats. In the present study, the spectral indices reduced to principal components using Principal Component Analysis (PCA), show a clear distinction between the sought differences in the data obtained from areas with different levels of pollution.

Between individual classes, the *CS* function provides higher separability results, which can be explained by the nature of the data and the different ways in which distance metrics process information. For classes with large differences in values (e.g. c1 and c4), the sqEuclidean distance works better. For classes with close scales but different orientations in space (c3 with the others), *CS* provides a clearer segregation due to the emphasis on angular differences.

In almost all cases of separability studied, the cityblock distance function does not capture the global structure of the data well, as a result of which it also indicates the lowest average value among the three distance functions.

The clustering performed between all defined classes simultaneously shows lower average values of the *S* criterion compared to the separability between individual pairs of classes. This result can be explained by the more complex structure of the data, leading to difficulties in defining clear boundaries between classes in conditions of high heterogeneity. These conditions increase the probability of overlap between clusters, which in turn has a negative impact on the overall separability between classes.

Dineva et al. [10] propose a method for determining the degree of air pollution using spectral characteristics of mulberry leaves, suitable for integration into mobile applications.

By optimising the classification algorithms based on kernel PCA and LDA to distinguish polluted and unpolluted areas, they achieve an error not exceeding 1 %. Although the mentioned methods offer more precise classification compared to the results obtained in the present study, they require significant computational resources, which is unjustified if the main goal is to quickly distinguish polluted and unpolluted areas in large urban spaces. As a limitation of the study, its focus on local pollution differentiation can also be indicated.

Correa-Ochoa et al. [36] also obtained data on air pollution through passive biomonitoring, including the use of 6 tree species. They used the APTI (Air Pollution Tolerance Index) and API (Anticipated Performance Index) indices to assess the resistance of plants to atmospheric pollutants and their potential for use as natural air filters.

The present study demonstrates the possibility of passively assessing air quality based on the condition of urban tree leaves. This approach directly addresses global challenges of urban air pollution, which remains a leading environmental health risk according to WHO and UNEP reports. Passive biomonitoring can complement conventional monitoring networks, especially in rapidly urbanising regions where infrastructure is limited. Future applications include integration into smart city platforms, citizen science programs for community-based monitoring, and long-term datasets that inform urban planning and public health policy.

The results of the present study highlight the importance of species specificity, which plays a significant role in the selection of appropriate bioindicators. The integrated approach based on spectral analysis, chemometric techniques and machine learning methods is an effective tool for assessing air quality and the environment, allowing the definition of areas with high and low pollution [37].

Mulberry and linden are tree species that respond to pollutants through changes in their anatomical and physiological properties, which can serve as indicators of environmental stress and environmental quality. However, the use of only two species represents a limitation, as leaf morphology, pollutant accumulation capacity, and physiological responses vary across species [38]. Seasonal factors such as leaf age, pigment composition, and moisture content may also influence spectral indices, potentially affecting classification accuracy [39]. Physiological variations related to growth stage or stress adaptation could further alter spectral responses [40]. Future studies should therefore expand the range of species and incorporate seasonal monitoring to strengthen the robustness and generalisability of passive biomonitoring approaches.

Conclusion

In this work, zones with strong and weak environmental pollution are defined from the point of view of passive bio-monitoring.

Four classes of zones with different degrees of environmental pollution are defined.

Spectral data for mulberry and linden leaves were collected in the four zones. It was found that their spectral indices, after reduced to three principal components using Principal Component Analysis, reflect different degrees of environmental pollution.

An assessment of the separability between classes was performed in order to accurately define zones with different degrees of pollution. The classification task was carried out using the Silhouette method, based on cluster analysis. The method using distance functions demonstrates significant potential for the application of machine learning techniques in environmental data analysis, resource management and pollution monitoring.

This study presents the possibility of passively determining the state of the environment depending on the state of the leaves of trees grown in urban environments. The results obtained will help create continuous monitoring programs to control the level of pollution and the impact of pollutants.

Acknowledgements

This study is technically and administrative supported by the project BG-RRP-2.004-0006-C02 “Development of scientific research and innovation at Trakia University in the service of health and sustainable well-being”.

References

[1] Manisalidis I, Stavropoulou E, Stavropoulos A, Bezirtzoglou E. Environmental and health impacts of air pollution: A review. Front Public Health. 2020;8:14. DOI: 10.3389/fpubh.2020.00014.

[2] Chen F, Zhang W, Bani Mfarrej MF, Saleem MH, Khan KA, Ma J, et al. Breathing in danger: Understanding the multifaceted impact of air pollution on health impacts. Ecotoxicol Environ Saf. 2024;280:116532. DOI: 10.1016/j.ecoenv.2024.116532.

[3] Nakhle P, Stamos I, Proietti P, Siragusa A. Environmental monitoring in European regions using the sustainable development goals (SDG) framework. Environ Sustain Indic. 2024;21:100332. DOI: 10.1016/j.indic.2023.100332.

[4] Ogidi OI, Onwuagba CG, Richard-Nwachukwu N. Biomonitoring tools, techniques and approaches for environmental assessments. In: Biomonitoring of Pollutants in the Global South. Chapter 7. 2024. DOI: 10.1007/978-981-97-1658-6_7.

[5] Wacławek M, Świsłowski P, Rajfur M. The biological monitoring as a source of information on environmental pollution with heavy metals. Chem Didact Ecol Metrol. 2022;27(1-2):53-78. DOI: 10.2478/cdem-2022-0006.

[6] Taurozzi D, Gallitelli L, Cesarini G, Romano S, Orsini M, Scalici M. Passive biomonitoring of airborne microplastics using lichens: A comparison between urban, natural and protected environments. Environ Int. 2024;187:108707. DOI: 10.1016/j.envint.2024.108707.

[7] Isinkaralar O, Świsłowski P, Isinkaralar K, Rajfur M. Moss as a passive biomonitoring tool for the atmospheric deposition and spatial distribution pattern of toxic metals in an industrial city. Environ Monit Assess. 2024;196:513. DOI: 10.1007/s10661-024-12696-x.

[8] Słonina N, Świsłowski P, Rajfur M. Passive and active biomonitoring of atmospheric aerosol with the use of mosses. Ecol Chem Eng S. 2021;28(2):163-72. DOI: 10.2478/eces-2021-0012.

[9] Zafarullah H, Huque AS. Climate change, regulatory policies and regional cooperation in South Asia. Public Adm Policy Asia-Pac J. 2018;21(1):22-35. DOI: 10.1108/PAP-06-2018-001.

[10] Dineva S, Veleva-Doneva P, Zlatev Z. Urban environmental quality assessment by spectral characteristics of Mulberry (Morus L.) leaves. Environments. 2021;8(9):87. DOI: 10.3390/environments8090087.

[11] Nebesnyi VB, Grodzynska GA. An assessment of industrial pollution of Kyiv with the spectral reflection of Tilia cordata (Tiliaceae) leaves. Ukr Bot J. 2015;72(2):116-21. DOI: 10.15407/ukrbotj72.02.116.

[12] Khavanin Zadeh AR, Veroustraete F, Buytaert JAN, Dirckx J, Samson R. Assessing urban habitat quality using spectral characteristics of Tilia leaves. Environ Pollut. 2013;178:7-14. DOI: 10.1016/j.envpol.2013.02.021

[13] Mielke MS, Schaffer B, Schilling AC. Evaluation of reflectance spectroscopy indices for estimation of chlorophyll content in leaves of a tropical tree species. Photosynthetica. 2012;50(3):343-52. DOI: 10.1007/s11099-012-0038-2

[14] Zhang Y, Wang C, Huang J, Wang F, Huang R, Lin H, et al. Exploring the optical properties of leaf photosynthetic and photo-protective pigments in vivo based on the separation of spectral overlapping. Remote Sens. 2020;12(21):3615. DOI: 10.3390/rs12213615.

[15] Yang L, Meng L, Gao H, Wang J, Zhao C, Guo M, et al. Heavy metal detection in mulberry leaves: Laser-induced breakdown spectroscopy data. Data Brief. 2020;33:106483. DOI: 10.1016/j.dib.2020.106483.

[16] Yu K, Van Geel M, Ceulemans T, Geerts W, Ramos M, Serafim C, et al. Vegetation reflectance spectroscopy for biomonitoring of heavy metal pollution in urban soils. Environ Pollut. 2018;243(Part B):1912-22. DOI: 10.1016/j.envpol.2018.09.053.
[17] Andrianjara I, Cabassa C, Lata J-C, Hansart A, Raynaud X, Renard M, et al. Characterization of stress indicators in Tilia cordata Mill. as early and long-term stress markers for water availability and trace element contamination in urban environments. Ecol Indic. 2024;158:111296. DOI: 10.1016/j.ecolind.2023.111296.
[18] Onwudiegwu CA, Sylva L, Aigberua AO, Hait M. Biological Monitoring of Air Pollutants. In: Izah SC, Ogwu MC, Shahsavani A, editors. Air Pollutants in the Context of One Health. The Handbook of Environmental Chemistry. Cham: Springer; 2024. vol. 134. DOI: 10.1007/698_2024_1139.
[19] Carlan I, Sandric I. The use of a field spectrometer and satellite imagery for identifying stressed vegetation in Bucharest, Romania. Int J Conserv Sci. 2020;11(1):125-32. Available from: https://www.proquest.com/scholarly-journals/use-field-spectrometer-satellite%20imagery/docview/2706213924/se-2.
[20] Huang L, Yang L, Meng L, Wang J, Li S, Fu X, et al. Potential of visible and near-infrared hyperspectral imaging for detection of Diaphania pyloalis larvae and damage on mulberry leaves. Sensors. 2018;18(7):2077. DOI: 10.3390/s18072077.
[21] Sultanova R, Martynova M, Odintsov G, Mukhamadiev D. Optical parameters of the Tilia cordata Mill. assimilation apparatus. Math Model Eng Probl. 2022;9(5):1187-91. DOI: 10.18280/mmep.090504.
[22] Ustin SL, Jacquemoud S. How the Optical Properties of Leaves Modify the Absorption and Scattering of Energy and Enhance Leaf Functionality. In: Cavender-Bares J, Gamon JA, Townsend PA, editors. Remote Sensing of Plant Biodiversity. Cham: Springer; 2020. DOI: 10.1007/978-3-030-33157-3_14.
[23] EPA. Environments and Contaminants - Criteria Air Pollutants. Available from: https://www.epa.gov/americaschildrenenvironment/environments-and-contaminants-criteria-air-pollutants.
[24] Lark R. Acceptable VOC Levels in PPM. Available from: https://environment.co/acceptable-voc-levels-ppm
[25] Bright RM, Lund MT. CO_2-equivalence metrics for surface albedo change based on the radiative forcing concept: A critical review. Atmos Chem Phys. 2021;21(12):9887-907. DOI: 10.5194/acp-21-9887-2021.
[26] Anderson K. Low-Emission Zone (LEZ): meaning, zones and restrictions. Available from: https://greenly.earth/en-us/blog/ecology-news/low-emission-zone-lez-meaning-zones-and-restrictions.
[27] James A. Can "Blue Zones" be a solution to environmental injustice? Available from: https://www.ehn.org/blue-zones-environmental-2658467593/what-are-blue-zones (accessed 2024 Jul 12).
[28] Latif SD, Almalayih M, Yafouz A, Ahmed AN, Zaini N, Irwan D, et al. Prediction of atmospheric carbon monoxide concentration utilizing different machine learning algorithms: A case study in Kuala Lumpur, Malaysia. Environ Technol Innov. 2023;32:103387. DOI: 10.1016/j.eti.2023.103387.
[29] Zlatev Z, Todorov A, Karadzhova D, Vasilev M, Veleva P. Evaluating the performance and practicality of a multi-parameter assessment system with design, comparative analysis, and future directions. Sustainability. 2024;16:4124:1-27. DOI: 10.3390/su16104124.
[30] Wyman C, Sloan P-P, Shirley P. Simple Analytic Approximations to the CIE XYZ Color Matching Functions. J Comput Graph Tech. 2013;2(2):1-11. Available from: https://jcgt.org/published/0002/02/01/.
[31] Atanassova S, Nikolov P, Valchev N, Masheva S, Yorgov D. Early detection of powdery mildew (Podosphaera xanthii) on cucumber leaves based on visible and near-infrared spectroscopy. AIP Conf Proc. 2019;2075:160014. DOI: 10.1063/1.5091341.
[32] Cermakova I, Komarkova J, Sedlak P. Calculation of Visible Spectral Indices from UAV-Based Data: Small Water Bodies Monitoring. In: 2019 14th Iberian Conference on Information Systems and Technologies CISTI; 2019. p. 1-5. DOI: 10.23919/CISTI.2019.8760609.
[33] Mladenov M. Model-based approach for assessment of freshness and safety of meat and dairy products using a simple method for hyperspectral analysis. J Food Nutr Res. 2020;59(2):108-19. Available from: https://www.vup.sk/en/download.php?bulID=2059.
[34] Silhouette plot. Available from: https://www.mathworks.com/help/stats/silhouette.html.
[35] Kaufman L, Rousseeuw PJ. Finding Groups in Data: An Introduction to Cluster Analysis. New York: Wiley; 1990. DOI: 10.1002/9780470316801.
[36] Correa-Ochoa M, Mejia-Sepulveda J, Saldarriaga-Molina J, Castro-Jiménez C, Aguiar-Gil D. Evaluation of air pollution tolerance index and anticipated performance index of six plant species, in an urban tropical valley: Medellin, Colombia. Environ Sci Pollut Res. 2021; 29(5):7952-71. DOI: 10.1007/s11356-021-16037-0.
[37] Konopka Z, Świsłowski P, Rajfur M. Biomonitoring of atmospheric aerosol with the use of Apis mellifera and Pleurozium schreberi. Chem Didact Ecol Metrol. 2019;24(1-2):107-16. DOI: 10.2478/cdem-2019-0009.
[38] Świsłowski P, Rajfur M. Mushrooms as biomonitors of heavy metals contamination in forest areas. Ecol Chem Eng S. 2018;25(4):557-68. DOI: 10.1515/eces-2018-0037.

[39] Świsłowski P, Kříž J, Rajfur M. The use of bark in biomonitoring heavy metal pollution of forest areas on the example of selected areas in Poland. Ecol Chem Eng S. 2020;27(2):195-210. DOI: 10.2478/eces-2020-0013.

[40] Słonina N, Świsłowski P, Rajfur M. Passive and active biomonitoring of atmospheric aerosol with the use of mosses. Ecol Chem Eng S. 2021;28(2):163-72. DOI: 10.2478/eces-2021-0012.